Polymer Chemistry

PET–RAFT polymerization catalyzed by cadmium selenide quantum dots (QDs): Grafting-from QDs photocatalysts to make polymer nanocomposites

SCHOLARONE™
Manuscripts

PET-RAFT polymerization catalyzed by cadmium selenide quantum dots (QDs): *Grafting-from* QDs photocatalysts to make polymer nanocomposites

Yifan Zhu[1] and Eilaf Egap*[1,2]

[1]Department of Materials Science and Nanoengineering and [2]Department of Chemical and Biomolecular Engineering, Rice University, Houston, Texas, 77005, United States

ABSTRACT: We report herein the first example of light-controlled radical reversible addition-fragmentation chain transfer (RAFT) polymerization facilitated by cadmium selenide (CdSe) quantum dots (QDs) as the photocatalyst and the *grafting-from* CdSe QDs nanoparticles to create polymer-QDs nanocomposites in a one pot photopolymerization. The CdSe QDs undergo a monophase ligand exchange with chain transfer agents (CTAs) via bithiol groups, enabling dispersion of CdSe in polar solvents as well as the grafting of CTAs on the surface of QDs. Photoinduced electron transfer (PET) between QDs and free CTAs facilitates the polymerization of multitude of functional monomers with temporal control, low dispersity ($Đ \approx$ 1.06), and high chain-end fidelity. More importantly, we leveraged CdSe QDs bound to CTAs to synthesize well-dispersed core-shell organic-inorganic polymer-QDs nanocomposites using a grafting-from polymerization approach.
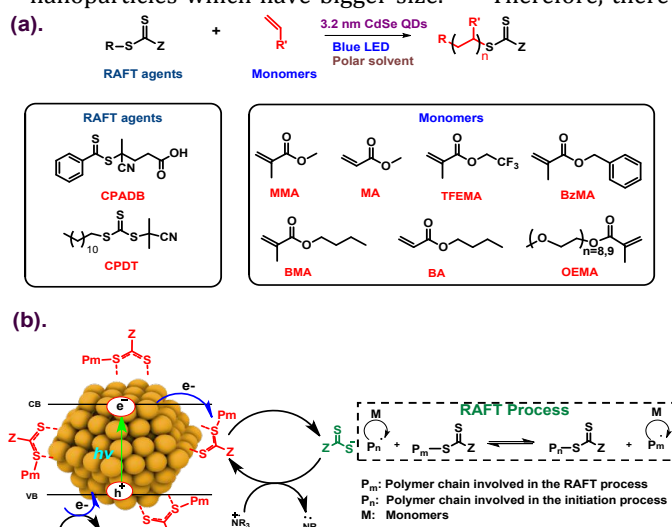
Recently, light-mediated control radical polymerizations (CRPs) have proven to be robust and powerful strategies to prepare well-defined polymers with complex architectures using mild reaction conditions with temporal control.[1-6] Light's renewability and sheer abundance properties make it one of the most promising external stimuli for remotely controlled living radical polymerization. Boyer,[7-13] Hawker,[14-18] Matyjaszewski,[3,6,19-22] Yagci,[23,24] Summerlin,[25,26] Qiao,[27-29] Tang[30] and Miyake[31-34] et al have successfully developed methodologies using a large scope of metal complexes[9,15] and organic small-molecule dyes[5] as photoinitiators or photocatalysts (PCs) and have even further employed these catalysts for macromolecular engineering.[35] Among all photo CRPs, light-mediated reversible addition-fragmentation chain transfer (RAFT) polymerization and atom transfer radical polymerization (ATRP) have gained significant attention and emerged as two of the most promising polymerization methodologies due to their applicability to a wide range of monomers, functional group tolerance, and ability to create tailor-made polymers.[1,2,5]

Both photo-mediated ATRP and RAFT polymerizations utilize photocatalysts (PCs) for electron transfer to active initiators (alkyl bromide or RAFT agents). Given this similar mechanism,[36] PCs with excited states that exhibit sufficient reductive potentials (<-0.7 V vs SCE)[33] can be successfully applied for both polymerizations. Indeed, Hawker[15,37] and Boyer[9] separately showcased that fac-tris(2-phenylpyridine)iridium can successfully polymerize methyl acrylates and methyl methacrylates through either ATRP or RAFT, providing polymers with tunable molecular weight (MW) and controlled molecular weight distribution. Furthermore, organic photocatalysts such as Eosin-Y have also proven to be effective for both ATRP and

RAFT polymerizations by Yagzi,[38] Summerlin,[26] and Boyer.[39] More recently, Miyake and Boyer reported organic photocatalyst, *N,N*-diarryl dihydrophenazines, to selectively mediate sequential ATRP and RAFT polymerizations to build block co-polymers.[36] These examples underscore the importance of developing PCs for both RAFT and ATRP polymerizations to provide significant opportunities for designing functional polymer structures and propels light-mediated polymerizations to the forefront.

Semiconductor quantum dots (QDs) are an emerging and novel class of PCs[40] because of their unique electrical and optical properties that arise from quantum confinement effects.[41,42] By modifying the QD surface, one can tailor the QD size, impacting the luminescence and band gap of the QD,[43] as well as improve dispersibility in the solvent or matrix.[42,44,45] Polymer-QDs nanocomposites are a well-studied example of surface modified QDs that have applications in optical/electrical sensors,[46] light emitting diodes,[47] and biological labeling / imaging.[48] Currently, synthesis of QD-polymer hybrid nanostructures largely depends on surface ligand exchange and modification. One can stabilize the QDs with ligands modified initiators and directly grow polymer from the QDs surface ("grafting from"),[49-51] or attach pre-synthesized polymers with functionalized end group to QDs via ligand exchange ("grafting to").[52] In general, grafting-from polymerization approach yields better control over surface polymer chain concentration and consequently polymerization effect compared to grafting-to.[45] However, current methods usually require extensive synthetic efforts and purification steps to gain modified ligands with initiators or polymers, and in addition, cumbersome secondary surface ligand exchange step are needed.[45] More importantly, most polymerizations are

1

driven by thermal initiation, which is not only energy inefficient but also raises the possibility that degradation of the QDs and modified ligand-initiator structures will occur at high temperatures.[51,53] With the robust development of photochemistry technology mentioned above, photo polymerization appears to be an alternative method for grafting polymer to the nanoparticle surface.[54–57] Indeed, in 2016, Matyjaszewski reported a surface initiated ATRP on silica using 10-phenylphenothiazine as the photocatalyst to prepare well-defined hybrid materials.[58] Very recently, Boyer and Lim have reported the very first example of directly growing polymer on lanthanide-doped up-conversion nanoparticles by using visible light mediated photoinduced electron transfer (PET) - RAFT polymerization.[59] Thickness of the polymer shell could easily be controlled by switching the light on and off. However, both of these examples require the use of external PCs that must be removed at the end of polymerization. Yin and coworkers reported a in situ photo-polymerization on TiO_2 nanoparticle surface where TiO_2 was also used as the photoinitiator,[55] but complicated surface modification are needed. Besides, considering the smaller size of QDs and agglomeration of QDs that usually occurs during the initiators grafting, functionalizing the surface of the QDs is more challenging compared to other nanoparticles which have bigger size.[45,60] Therefore, there

(a).

RAFT agents

CPADB

CPDT

Monomers

MMA   MA   TFEMA   BzMA

BMA   BA   OEMA

(b).

RAFT Process

P_m: Polymer chain involved in the RAFT process
P_n: Polymer chain involved in the initiation process
M: Monomers

is a need to explore various methods for synthesizing functional QDs polymeric nanocomposites.

Figure 1. (a) PET-RAFT polymerization with various monomers and RAFT agents driven by blue LED light (10 mW/cm^2) at 25 °C in the presence of CdSe QD as the photocatalyst (b) Proposed mechanism of CdSe QDs-catalyzed PET-RAFT polymerization. Dash lines stand for dynamic bonds; NR$_3$ stands for DIPEA

Herein, we report the first example of RAFT polymerization facilitated by CdSe QDs as the photocatalyst and the *grafting-from* photocatalyst nanoparticles to create well-dispersed polymer-QDs nanocomposites in a one pot photopolymerization (Figure 1). We[61] and others[62,63] have previously demonstrated CdSe QDs as effective photoredox catalysts for light mediated ATRP and free radical polymerization, thus we hypothesized that CdSe QDs* excited-state that has a

strong reducing potential (-1.59 V vs SCE) to mediate PET-RAFT polymerization via a similar electron transfer mechanism as ATRP (Figure 1). Inspired by previous studies that demonstrated strong affinities of RAFT agent end groups (typically di- and trithio compounds) toward gold nanoparticles,[64,65] we foresaw that RAFT agents would have an affinity to CdSe QDs surface and partially substitute the original ligands.[66,67] Indeed, we find that RAFT agents decorate the surface of CdSe QDs, thus allowing both the initiation and propagation steps of the polymer chain from the surface of CdSe QDs, while simultaneously maintaining the dual role of the CdSe QDs as the photocatalyst and as the inorganic nanocomposite. We also elucidated the role of solvents, catalyst loading, RAFT agent feed ratio, different monomers as well as polymerization kinetics. Furthermore, transmission electron microscope (TEM) clearly showed the formation of a well dispersed polymers-CdSe QDs nanocomposites after polymerization. To the best of our knowledge, there are only two examples using nanomaterials as photocatalysts for PET-RAFT polymerization,[21,68] and there is no example using photopolymerization in preparing polymer-coated QDs or hybrid core-shell organic/inorganic polymeric materials in one-step/one pot.

We initially employed a ligand-exchange strategy that enables both phase transfer of oleic acid (OA) capped CdSe (3.2 nm) from a non-polar solvent (hexane) to a polar solvent dimethylformamide (DMF). Briefly, the RAFT agent (4-cyano-4-(phenylcarbonothioylthio) pentanoic acid (CPADB)), methyl methacrylate (MMA) monomer, and OA capped CdSe QDs were mixed together for 5 minutes. After the addition of polar solvent DMF, a clear solution was yield. In contrast, directly adding the OA capped QDs into DMF led to the aggregation of QDs (Figure S2). This likely indicates that there is a monophase ligand exchange mechanism between the OA capped CdSe QDs and the CPADB in MMA. We hypothesize that the bithiol group in CPABD binds with the QDs surface via Lewis acid-base interaction[66,67] to displace the original ligand (i.e. OA) while the carboxylic acid group helps to dissolve the CdSe QDs in polar solvents. The advantage of this monophase ligand exchange in MMA lies in its generality, simplicity and without altering the size or optical properties of QDs.[69] Indeed, UV-vis and fluorescence spectra show a minor blue shift in the first excitonic peak of QDs by about 4 nm after grafting RAFT agent onto CdSe QDs (Figure S3), indicting QDs surface is intact after ligand exchange.

Surface modification of CdSe QDs with CPADB was confirmed using nuclear magnetic resonance (NMR) spectroscopy and fourier transform infrared (FTIR) spectroscopy. To ensure that all CPADB signal was from CPADB grafted onto the QDs, the reaction mixture was washed with methanol and centrifuged to obtain the QDs precipitate. FTIR spectrum of the CPADB grafted QDs (Figure S4) shows a characteristic absorption band at 2242 cm^{-1} which is attributed to the cyano group on CPADB, indicative of grafted CPADB onto the surface of CdSe QDs. In addition, the peak observed around 3500 cm^{-1} can be attributed to solvated water molecules, consistent with the hydrophilicity of the QDs after ligand exchange.[70] ^{1}H NMR of the CPADB grafted QDs (Figure S5) shows several broad

2

peaks around 7.8 ppm, 7.5 ppm, and 7.3 ppm which correspond to the benzyl hydrogens in CPADB. Notably, both ^{1}H NMR and

Table 1. CdSe QDs catalyzed PET-RAFT polymerizations in DMF under blue LED (λ_{max} = 465 nm) irradiation

Entry	Monomer	[M]:[CTA]:[DIPEA] [a]	[QD] (ppm)	Conversion(%)[b]	M_n (kDa)[c]	Đ	$M_{n,theo}$ (kDa)[d]
1	MMA	200:1:5	15	55.6	16.6	1.09	11.5
2[e]	MMA	200:1:5	15	0	/	/	/
3	MMA	200:1:5	0	7.7	/	/	/
4	MMA	200:1:0	15	9.2	/	/	/
5[f]	MMA	200:1:5	15	50.0	20.6	1.12	10.3
6	MMA	200:1:5	30	60.3	19.3	1.07	12.3
7	MMA	200:1:5	45	63.4	20.1	1.06	12.9
8	MMA	200:1:5	7	33.2	50.4	1.37	6.9
9	MMA	200:1:15	15	54.5	15.8	1.14	11.1
10	MMA	200:1:10	15	53.6	16.4	1.14	10.9
11	MMA	200:1:2.5	15	56.3	17.0	1.10	11.4
12	BzMA	200:1:5	15	77.0	31.0	1.13	27.4
13	OEMA	100:1:5	15	92.3	45.7	1.24	46.4
14	MA	200:1:5	15	76.7	12.2	1.09	13.3
15	BA	200:1:5	15	86.3	20.0	1.12	22.3

[a]. CTA for entry 1 to 14 is CPADB and entry 15 to 16 is CPDT; reaction time is 24 hours unless otherwise specified.[b]. Conversion measured by ¹HNMR. [c]. Mn measured by GPC in THF, based on linear polystyrene as calibration standard. [d]. $M_{n, theo}$ = [monomer]/[initiator] × conversion× MW (monomer) + MW (initiator) [e]. polymerization was conducted in the dark [f]. polymerization was conducted in air

FTIR show residual oleic acid on the QDs. We should note that, RAFT grafted CdSe QDs solutions used for polymerization also contains unbound RAFT agents. This may facilitate enhanced control of surface initiated polymerization due to the enhanced chain transfer efficiency.[59] Furthermore, QDs after ligand exchange seemed relatively stable and well-dispersed for at least two days, as no inter-particle coupling/ aggregation is observed on the transmission electron microscopy (TEM) images (Figure S6) of CPADB capped QDs. Similarly, the dynamic light scattering (DLS) spectrum (Figure S7) of the CPADB capped QDs shows a mono-dispersed size distribution (mean size of 3.8 nm), suggesting no aggregation as a result of ligand exchange.

Once the grafting of CPADB onto the surface of CdSe QDs was established, we sought to evaluate the viability of CPADB- capped CdSe QD-mediated RAFT polymerization in DMF with an external electron donor *N*, *N*-Diisopropylethylamine (DIPEA) under blue light irradiation (460-480 nm) for 24 hours (Table 1, entry 1). Encouragingly, the reaction achieved 55.6% monomer conversion, resulting in a polymer with a molecular weight of 16.6 KDa and a dispersity (Đ) of only 1.09. To prove the necessity of each reaction component, such as light, QDs catalyst, and DIPEA, control experiments were performed by eliminating one component at a time. Not surprisingly, in the absence of photo-irradiation (entry 2), the polymerization does not proceed, indicative of a photo-

induced polymerization. Lack of CdSe QDs (entry 3) results in a monomer conversion of only 7.7% after 24 hours of illumination under blue light in DMF, clearly demonstrating a photomediated polymerization catalyzed by CdSe QDs. In the absence of external electron donor, DIPEA, (entry 4), only 9.2% monomer conversion was reached, consistent with our previous work.[61] We propose that the sacrificial electron donor, DIPEA, acts as a hole scavenger for the QDs excited state and minimizes back electron transfer, thus promoting PET and improving catalyst turnover.[71] It is noteworthy to mention that this reaction proceeds in air in a controlled fashion (entry 5), resulting in a slightly lower monomer conversion of 50.0% compared to degassed procedure (55.6%) with a low Đ = 1.12. We find that the polymerization proceeds under the irradiation of green LED (λ_{max} =535 nm, light intensity 10 mW/cm²), albeit with low monomer conversion (27.2%, Table S1) compared to that of a blue LED (55.6%) (Table 1, entry 1). This is not surprising given the strong absorption of CdSe QDs in the blue region (λ_{max} =465 nm) compared to that of green light region (λ_{max} =535 nm), Figure S3.

We further elucidated the effect of solvent polarity on polymerization by examining various polar solvents such as dimethyl sulfoxide (DMSO), *N,N*-dimethylacetamide (DMA), acetonitrile (MeCN) and a non-polar solvent such as toluene (Table S1, entry 1-4). In general, high monomer conversion was achieved in polar solvents compared to non-polar or relatively less-polar solvents. This is

4

consistent with photoinduced polymerization mechanism where polar solvents stabilize charge-separated species and a fast electron transfer favors the initiation step.[1] For example, in DMSO, a higher monomer conversion of 77.3% was achieved after 24 hours compared to 55.6 % in DMF, and a low Đ 1.13 was maintained. This is likely due to the fact that the dielectric constant of DMSO (46.7) is higher than that of DMF (37.8), permitting faster electron transfer. However, we observed polymerization in DMSO exhibited a big deviation between theoretical (15.7 KDa) and experimental (30.3 KDa) molecular weight, presumably, due to radical recombination of dead chains. Polymerization in DMA which has similar polarity to DMF, gives Đ as low as 1.12 and a moderate monomer conversion of 49.4%. Poor monomer conversion of 30.1% in MeCN is observed and attributed to the poor solubility of CdSe QDs in MeCN. On the other hand, polymerization in non-polar solvent such as toluene results in a precipitation of QDs and trace amount polymers. These results suggest that a good QDs-CPABD solubility is crucial to obtain well-defined final polymer product.

The effect of catalyst loadings on the polymerization was further probed. In principle, a higher reaction rate should be achieved without influencing the Đ and M_n as a result of an increase in the catalyst concentration above a critical value. As such, an increase in the QDs loading from 15 ppm to 30 ppm in DMF resulted in an increase in the monomer conversion from 55.6% to 60.3%, respectively, with no significant difference in Đ (1.07) within the same experimental time frame (Table 1, entry 1 and 6). Further increase in a catalyst loading of 45 ppm, gave a monomer conversion increase up to 63.4% with a low Đ of 1.06 (entry 7). These results confirm that CdSe QDs act as a catalyst instead of a stoichiometric reagent. However, at a relatively low catalyst loading of 7 ppm (entry 8), polymerization does not proceed in a controlled manner and yields a relatively high Đ of 1.37. It is possible that a higher concentration of QDs enhances the activation rate and efficiently reduces the RAFT agent as a result of an increase in excited state QDs, which leads to a higher conversion.[72]

We systematically varied the ratio of the DIPEA with respect to the monomer, [MMA]:[DIPEA] ranging from 200:2.5 to 200:15 (Table 1, entry 1, 9 and 10) to investigate its role in this polymerization. Despite a successive increase of the DIPEA concentration, the monomer conversion remained consistent at around 55% without any change in the M_n and a consistent Đ of 1.1. These results clearly eliminate the possibility of DIPEA acting as an initiator or co-initiator. However, at a ratio of 200:1.25 of [MMA] to [DIPEA] or below (Table 1, entry 11 and Table S1), reaction became sluggish with a monomer conversion of 40% or less after 24 hours. It is possible that higher amine concentration, initial traps on quantum dots were saturated with DIPEA, which can promote a higher efficiency of hole transfer from quantum dots to amine.[73] On the other hand, varying the [MMA]:[RAFT] agent ratio successfully provided PMMA polymers with tunable molecular weights, proving that RAFT agent/chain transfer agent (CTA) is the initiating species. An increase in the ratio of monomer to CTA from 400:1 to 100:1 (Table S1), leads to an increase in the monomer conversion from

39.3% to 68.0% within 24 hours, presumably due to faster initiation rate.

To test the versatility of the QD-mediated RAFT system, we screened a broad scope of functional methacrylates and acrylates monomers (Table 1, entry 12 - 15; Table S1). Satisfyingly, we found that all of the functional methacrylates and acrylates can undergo controlled polymerization in the presence of CPADB and CdSe QDs. For example, both benzyl methacrylate (BzMA) and butyl methacrylate (BMA) gave well-defined polymers with narrow molecular weight distribution (1.13 and 1.29, respectively) and excellent agreements between experimental and theoretical M_n (Table 1, entries 12 and 15). Functional fluorinated methacrylate, 2,2,2-trifluoroethyl methacrylate (TFEMA), was successfully polymerized using CdSe QDs as a photocatalyst with a conversion of 46.2%, and Đ of 1.25 after 24 hours irradiation. We further expanded this system and tested water soluble monomers such as oligo-(ethylene glycol) methyl ether methacrylate (OEMA), which after 24 hours resulted in 92.3% conversion and precision control over polymer molecular weight was achieved ($M_{n,theo}$= 46.4 KDa, $M_{n,GPC}$ = 45.7KDa).
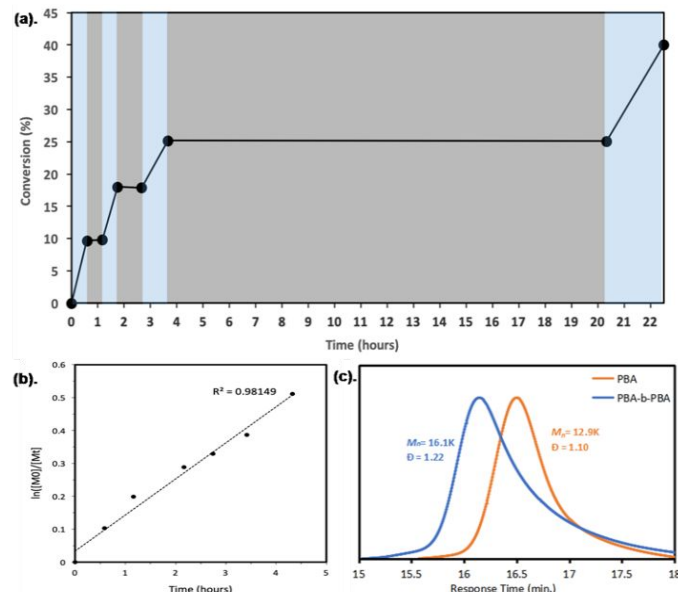
Figure 2. (a). Polymerization of MMA using CdSe QDs with repeated "on–off" cycling of the reaction to light; blue color means "light on"; grey color means "light off" (b). First-order kinetic analysis of the PET-RAFT polymerization of MMA in DMSO using CdSe QDs (c). In situ chain extension of PBA.

In order to expand the starting materials to acrylates monomers, the trithiol compound 2-cyano-2-propyl dodecyl trithiocarbonate (CPDT) was utilized instead. Not surprisingly, monomers such as methyl acrylates (MA) and butyl acrylates (BA) were successfully polymerized (Table 1, entry 14 and 15), achieving 76.7% and 86.3% conversion, respectively, after 24 hours irradiation, producing polymers with Đ as low as 1.09. In order to rule out the possibility that the polymerization was initiated by photolysis of the carbon–sulfur (C–S) bond,[28,29] control study was carried out in the absence of QDs (Table S1). Encouragingly, much lower conversion for both MA and BA (13.0% and 30.2%, respectively) was obtained with the

same irradiation time, indicting CdSe QDs mediated PET mechanism is dominant in the polymerization of acrylate monomers with CPDT.

To investigate the mechanism of the PET-RAFT facilitated by CdSe QDs, we performed a range of kinetic studies. Temporal control was confirmed by conducting polymerizations of MMA with intermittent light irradiation. Switching the light OFF halted the reaction completely while switching the light ON resumed the linear propagation (Figure 2a). Notably, no conversion was observed even after a 17 hours dark time, demonstrating the ability of QDs to remain dormant for a long time and maintain nice temporal control over polymerization process.[74] A plot of $\ln([M]_0/[M]_t)$ versus total exposure time follows a linear relationship and a pseudo first-order kinetics (Figure 2b). These results prove that in the absence of light, the polymerization stops and without activation of the chain ends. It is worthwhile to mention that both temporal control and first order kinetics were also observed in the presence of oxygen (Figure S8 and S9), albeit with slower reaction rates. To further confirm the presence of CTA end groups on the polymer, purified PMMA polymers were analyzed by ^{1}H NMR and GPC. The chemical shifts of δ= 7.4, 7.6, and 7.8 ppm in the ^{1}H NMR spectrum are attributed to the phenyl group in CPADB (Figure S10). Both UV (λ = 350 nm) and RI detectors showed similar GPC trace (Figure S11), MW and Đ, suggesting the presence of the dithiobenzoate end-group. To further investigated the end-group fidelity, in situ chain extension of PBA and PMMA were carried using BA and MMA monomers to obtain diblock copolymers: PBA-*b*-PBA and PMMA-*b*-PMMA (Scheme S1). The diblock copolymerizations were obtained by sequential monomer addition in one pot, which mitigates the need for elaborate polymer purification to afford efficient chain extension. The GPC shows a shift of macroinitiators to lower retention time with formation of well-defined blocks with low Đ (1.10 and 1.11), suggesting an excellent chain-end fidelity (Figures 2b and S12). Based on all the above results, we propose that under light irradiation, photoexcited CdSe QDs react with either grafted-RAFT on surface of CdSe QDs or unbound RAFT agents in the solution via PET process while holes in valence band of CdSe can be scavenged by sacrificial donors DIPEA (Figure 1b). Reduced RAFT agents play a dual role as both the initiators and degenerative chain transfer agents. Radicals generated by reduced RAFT agent can initiate the polymerizations, participate in RAFT process or be deactivated by either DIPEA radical cation[26] or excited QDs[17] to form a dormant state polymer. An efficient exchange of unbound or free RAFT agent and grafted RAFT agent facilitates the chain propagation and prevents interparticle coupling, eventually leading to a good control over polymerization.[59] Considering the low loading of CdSe QDs, large amount of free polymer should be produced and meanwhile polymer could also be grafted onto QDs through RAFT agent attached to the particle surface.

To confirm QDs-polymer hybrid nanostructures were successfully synthesized via grafting-from approach, transmission electron microscopy (TEM) was used to analyze the reaction mixture composite. As both the matrix and the polymer brush grafted on the QDs have the same

6

chemical structure, nanocomposite should be miscible with matrix, and hence spatial dispersion.[49,50] Indeed, TEM images revealed that QDs are uniformly dispersed throughout the BzMA polymer matrix as well as PMMA polymer matrix in a non-aggregated fashion (Figure 3), suggesting a successful grafting of polymer on the nanoparticles.
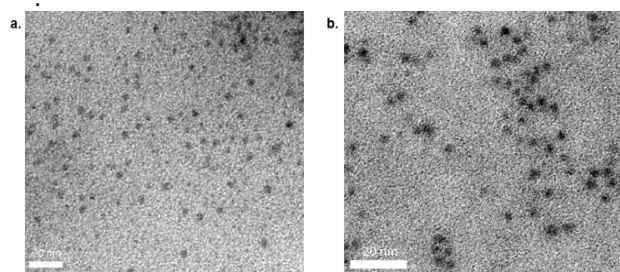
Figure 3. TEM images of (a). PBzMA covered CdSe QDs in PBzMA matrix (M_n= 31.6 KDa) (b). PMMA covered CdSe QDs in PMMA matrix (M_n= 3.6 KDa)

In conclusion, a highly efficient visible-light-regulated RAFT polymerization using CdSe QDs as photocatalysts was presented. Various functional polymers with moderate to excellent control and low dispersity were successfully polymerized. We show that CdSe QDs–catalyzed PET-RAFT polymerization exhibits good temporal control with high chain end fidelity polymers. Moreover, a *grafting-from* polymerization approach is achieved in one pot procedure because RAFT agents can bind to the surface of CdSe QDs to synthesize core-shell organic-inorganic polymer-coated QDs nanocomposites. The advantages of this strategy lie in its highly responsive approach, low catalyst loading, excellent and diverse functional tolerance, facile one-pot synthesis, tolerance to oxygen, simplicity and versatility in tuning QDs redox and electronic properties, and integration of nanomaterials for fabrication of hybrid organic/inorganic systems. We foresee that this *"one stone two birds approach"* where CdSe plays a dual role as both the photocatalyst and the inorganic building block for nanoparticle-polymer hybrid nanocomposites will expand the toolbox for the creation of complex polymer architectures and hybrid nanomaterials.

ASSOCIATED CONTENT

The Supporting Information is available free of charge via the Internet at http://pubs.acs.org."

AUTHOR INFORMATION

Corresponding Author

*Email: ee30@rice.edu

Notes

There are no conflicts to declare

ACKNOWLEDGMENT

REFERENCES

1 M. Chen, M. Zhong and J. A. Johnson, *Chem. Rev.*, 2016, **116**, 10167–10211.

2 N. Corrigan, S. Shanmugam, J. Xu and C. Boyer, *Chem. Soc. Rev.*, 2016, **45**, 6165–6212.

3 T. G. Ribelli, D. Konkolewicz, X. Pan and K. Matyjaszewski, *Macromolecules*, 2014, **47**, 6316–6321.

4 J. C. Theriot, B. G. McCarthy, C.-H. Lim and G. M. Miyake, *Macromol. Rapid Commun.*, 2017, **38**, 1700040.

5 E. H. Discekici, A. Anastasaki, J. Read de Alaniz and C. J. Hawker, *Macromolecules*, 2018, **51**, 7421–7434.

6 X. Pan, M. A. Tasdelen, J. Laun, T. Junkers, Y. Yagci and K. Matyjaszewski, *Prog. Polym. Sci.*, 2016, **62**, 73–125.

7 S. Shanmugam, J. Xu and C. Boyer, *J. Am. Chem. Soc.*, 2015, **137**, 9174–9185.

8 S. Shanmugam, J. Xu and C. Boyer, *Macromolecules*, 2014, **47**, 4930–4942.

9 J. Xu, K. Jung, A. Atme, S. Shanmugam and C. Boyer, *J. Am. Chem. Soc.*, 2014, **136**, 5508–5519.

10 J. Yeow, O. R. Sugita and C. Boyer, *ACS Macro Lett.*, 2016, **5**, 558–564.

11 J. Xu and C. Boyer, *Macromolecules*, 2015, **48**, 520–529.

12 J. Xu, K. Jung, N. A. Corrigan and C. Boyer, *Chem. Sci.*, 2014, **5**, 3568.

13 S. Shanmugam, J. Xu and C. Boyer, *Chem. Sci.*, 2015, **6**, 1341–1349.

14 J. Niu, D. J. Lunn, A. Pusuluri, J. I. Yoo, M. A. O'Malley, S. Mitragotri, H. T. Soh and C. J. Hawker, *Nat. Chem.*, 2017, **9**, 537–545.

15 B. P. Fors and C. J. Hawker, *Angew. Chemie Int. Ed.*, 2012, **51**, 8850–8853.

16 J. E. Poelma, B. P. Fors, G. F. Meyers, J. W. Kramer and C. J. Hawker, *Angew. Chemie - Int. Ed.*, 2013, **52**, 6844–6848.

17 J. Niu, Z. A. Page, N. D. Dolinski, A. Anastasaki, A. T. Hsueh, H. T. Soh and C. J. Hawker, *ACS Macro Lett.*, 2017, **6**, 1109–1113.

18 N. J. Treat, H. Sprafke, J. W. Kramer, P. G. Clark, B. E. Barton, J. Read de Alaniz, B. P. Fors and C. J. Hawker, *J. Am. Chem. Soc.*, 2014, **136**, 16096–16101.

19 X. Pan, C. Fang, M. Fantin, N. Malhotra, W. Y. So, L. A. Peteanu, A. A. Isse, A. Gennaro, P. Liu and K. Matyjaszewski, *J. Am. Chem. Soc.*, 2016, **138**, 2411–2425.

20 D. Konkolewicz, K. Schröder, J. Buback, S. Bernhard and K. Matyjaszewski, *ACS Macro Lett.*, 2012, **1**, 1219–1223.

21 J. Jiang, G. Ye, Z. Wang, Y. Lu, J. Chen and K. Matyjaszewski, *Angew. Chemie Int. Ed.*, 2018, **57**, 12037–12042.

22 X. Pan, M. Lamson, J. Yan and K. Matyjaszewski, *ACS Macro Lett.*, 2015, **4**, 192–196.

23 C. Kutahya, A. Allushi, R. Isci, J. Kreutzer, T. Ozturk, G. Yilmaz and Y. Yagci, *Macromolecules*, 2017, **50**, 6903–6910.

24 A. Allushi, S. Jockusch, G. Yilmaz and Y. Yagci, *Macromolecules*, 2016, **49**, 7785–7792.

25 B. S. Tucker, M. L. Coughlin, C. A. Figg and B. S. Sumerlin, *ACS Macro Lett.*, 2017, **6**, 452–457.

26 C. A. Figg, J. D. Hickman, G. M. Scheutz, S. Shanmugam, R. N. Carmean, B. S. Tucker, C. Boyer and B. S. Sumerlin, *Macromolecules*, 2018, **51**, 1370–1376.

27 Q. Fu, Q. Ruan, T. G. McKenzie, A. Reyhani, J. Tang and G. G. Qiao, *Macromolecules*, 2017, **50**, 7509–7516.

28 Q. Fu, K. Xie, T. G. McKenzie and G. G. Qiao, *Polym. Chem.*, 2017, **8**, 1519–1526.

29 T. G. McKenzie, Q. Fu, E. H. H. Wong, D. E. Dunstan and G. G. Qiao, *Macromolecules*, 2015, **48**, 3864–3872.

30 J. Wang, L. Yuan, Z. Wang, M. A. Rahman, Y. Huang, T. Zhu, R. Wang, J. Cheng, C. Wang, F. Chu and C. Tang, *Macromolecules*, 2016, **49**, 7709–7717.

31 C. H. Lim, M. D. Ryan, B. G. McCarthy, J. C. Theriot, S. M. Sartor, N. H. Damrauer, C. B. Musgrave and G. M. Miyake, *J. Am. Chem. Soc.*, 2017, **139**, 348–355.

32 G. M. Miyake and J. C. Theriot, *Macromolecules*, 2014, **47**, 8255–8261.

33 J. C. Theriot, C.-H. Lim, H. Yang, M. D. Ryan, C. B. Musgrave and G. M. Miyake, *Science (80-.).*, 2016, **352**, 1082–1086.

34 D.-F. Chen, B. M. Boyle, B. G. McCarthy, C.-H. Lim and G. M. Miyake, *J. Am. Chem. Soc.*, 2019, **141**, 13268–13277.

35 K. Matyjaszewski and N. V. Tsarevsky, *J. Am. Chem. Soc.*, 2014, **136**, 6513–6533.

36 J. C. Theriot, G. M. Miyake and C. A. Boyer, *ACS Macro Lett.*, 2018, **7**, 662–666.

37 N. J. Treat, B. P. Fors, J. W. Kramer, M. Christianson, C.-Y. Chiu, J. Read de Alaniz and C. J. Hawker, *ACS Macro Lett.*, 2014, **3**, 580–584.

38 C. Kutahya, F. S. Aykac, G. Yilmaz and Y. Yagci, *Polym. Chem.*, 2016, **7**, 6094–6098.

39 J. Xu, S. Shanmugam, H. T. Duong and C. Boyer, *Polym. Chem.*, 2015, **6**, 5615–5624.

40 M. S. Kodaimati, K. P. McClelland, C. He, S. Lian, Y. Jiang, Z. Zhang and E. A. Weiss, *Inorg. Chem.*, 2018, **57**, 3659–3670.

41 A. P. Alivisatos, *J. Phys. Chem.*, 1996, 100, 13226–13239.

42 A. M. Smith and S. Nie, *Acc. Chem. Res.*, 2010, **43**, 190–200.

43 J. Lee, V. C. Sundar, J. R. Heine, M. G. Bawendi and K. F. Jensen, *Adv. Mater.*, 2000, **12**, 1102–1105.

44 A. M. Smith, H. Duan, M. N. Rhyner, G. Ruan and S. Nie, *Phys. Chem. Chem. Phys.*, 2006, **8**, 3895.

45 N. Tomczak, R. Liu and J. G. Vancso, *Nanoscale*, 2013, **5**, 12018.

46 I. Potapova, R. Mruk, C. Hübner, R. Zentel, T. Basché and A. Mews, *Angew. Chemie - Int. Ed.*, 2005, **44**, 2437–2440.

47 H. Skaff, K. Sill and T. Emrick, *J. Am. Chem. Soc.*, 2004, **126**, 11322–11325.

48 W. C. W. Chan and S. Nie, *Science (80-.).*, 1998, **281**, 2016–2018.

49 A. C. C. Esteves, L. Bombalski, T. Trindade, K. Matyjaszewski and A. Barros-Timmons, *Small*, 2007, **3**, 1230–1236.

50 H. Skaff and T. Emrick, *Angew. Chemie*, 2004, **116**, 5497–5500.

51 A. C. C. Esteves, P. Hodge, T. Trindade and A. M. M. V. Barros-Timmons, *J. Polym. Sci. Part A Polym. Chem.*, 2009, **47**, 5367–5377.

52 M. S. Nikolic, M. Krack, V. Aleksandrovic, A. Kornowski, S. Förster and H. Weller, *Angew. Chemie Int. Ed.*, 2006, **45**, 6577–6580.

53 C. Boyer, V. Bulmus, P. Priyanto, W. Y. Teoh, R. Amal and T. P. Davis, *J. Mater. Chem.*, 2009, **19**, 111–123.

54 J. Yan, B. Li, F. Zhou and W. Liu, *ACS Macro Lett.*, 2013, **2**, 592–596.

55 X. Wang, Q. Lu, X. Wang, J. Joo, M. Dahl, B. Liu, C. Gao and Y. Yin, *ACS Appl. Mater. Interfaces*, 2016, **8**, 538–546.

56 T. Ding, J. Mertens, A. Lombardi, O. A. Scherman and J. J. Baumberg, *ACS Photonics*, 2017, **4**, 1453–1458.

57 A. Bagheri, Z. Sadrearhami, N. N. M. Adnan, C. Boyer and M. Lim, *Polymer (Guildf).*, 2018, **151**, 6–14.

58 J. Yan, X. Pan, M. Schmitt, Z. Wang, M. R. Bockstaller and K. Matyjaszewski, *ACS Macro Lett.*, 2016, **5**, 661–665.

59 A. Bagheri, H. Arandiyan, N. N. M. Adnan, C. Boyer and M. Lim, *Macromolecules*, 2017, **50**, 7137–7147.

60 C. Boyer, M. H. Stenzel and T. P. Davis, *J. Polym. Sci. Part A Polym. Chem.*, 2011, **49**, 551–595.

61 Y. Huang, Y. Zhu and E. Egap, *ACS Macro Lett.*, 2018, **7**, 184–189.

62 N. C. Strandwitz, A. Khan, S. W. Boettcher, A. A. Mikhailovsky, C. J. Hawker, T.-Q. Nguyen and G. D. Stucky, *J. Am. Chem. Soc.*, 2008, **130**, 8280–8288.

63 A. A. Pawar, S. Halivni, N. Waiskopf, Y. Ben-Shahar, M. Soreni-Harari, S. Bergbreiter, U. Banin and S. Magdassi, *Nano Lett.*, 2017, **17**, 4497–4501.

64 C. Boyer, M. R. Whittaker, M. Luzon and T. P. Davis, *Macromolecules*, 2009, **42**, 6917–6926.

65 A. S. Duwez, P. Guillet, C. Colard, J. F. Gohy and C. A. Fustin, *Macromolecules*, 2006, **39**, 2729–2731.

66 S. Lian, D. J. Weinberg, R. D. Harris, M. S. Kodaimati and E. A. Weiss, *ACS Nano*, 2016, **10**, 6372–6382.

67 R. D. Harris, V. A. Amin, B. Lau and E. A. Weiss, *ACS Nano*, 2016, **10**, 1395–1403.

68 E. Liang, M. Liu, B. He and G.-X. Wang, *Adv. Polym. Technol.*, 2018, **37**, 2879–2884.

69   M. Q. Dai and L. Y. L. Yung, *Chem. Mater.*, 2013, **25**, 2193–2201.

70   C. Li, J. Han, C. Y. Ryu and B. C. Benicewicz, *Macromolecules*, 2006, **39**, 3175–3183.

71   A. K. Simlandy, B. Bhattacharyya, A. Pandey and S. Mukherjee, *ACS Catal.*, 2018, **8**, 5206–5211.

72   M. D. Ryan, R. M. Pearson, T. A. French and G. M. Miyake, *Macromolecules*, 2017, **50**, 4616–4622.

73   C. Landes, C. Burda, M. Braun and M. A. El-Sayed, *J. Phys. Chem. B*, 2001, **105**, 2981–2986.

74   N. D. Dolinski, Z. A. Page, E. H. Discekici, D. Meis, I. Lee, G. R. Jones, R. Whitfield, X. Pan, B. G. McCarthy, S. Shanmugam, V. Kottisch, B. P. Fors, C. Boyer, G. M. Miyake, K. Matyjaszewski, D. M. Haddleton, J. R. Alaniz, A. Anastasaki and C. J. Hawker, *J. Polym. Sci. Part A Polym. Chem.*, 2019, **57**, 268–273.